

# Stiffening and ventricular–arterial interaction in the ascending aorta using MRI: ageing effects in healthy humans

Ye Li<sup>a,c</sup>, Stacey S. Hickson<sup>b</sup>, Carmel M. McEnery<sup>b</sup>, Ian B. Wilkinson<sup>b</sup>, and Ashraf W. Khir<sup>c</sup>

**Objectives:** The aim of this study was to investigate the effect of age and sex on  $n$ PWV and  $n$ dI in the ascending aorta of healthy humans.

**Background:** Local pulse wave velocity ( $n$ PWV) and wave intensity ( $n$ dI) in the human ascending aorta have not been studied adequately, because of the need for invasive pressure measurements. However, a recently developed technique made the noninvasive determination of  $n$ PWV and  $n$ dI possible using measurements of flow velocity and arterial diameter.

**Methods:** Diameter and flow velocity were measured at the level of the ascending aorta in 144 healthy participants (aged 20–77 years, 66 men), using MRI.  $n$ PWV,  $n$ dI parameters; forward (FCW); backward (BCW) compression waves, forward decompression wave (FDW), local aortic distensibility ( $n$ D<sub>s</sub>) and reflection index ( $n$ RI) were calculated.

**Results:**  $n$ PWV increased significantly with age from  $4.7 \pm 0.3$  m/s for those 20–30 years to  $6.4 \pm 0.2$  m/s for those 70–80 years ( $P < 0.001$ ) and did not differ between sexes.  $n$ D<sub>s</sub> decreased with age ( $5.3 \pm 0.5$  vs.  $2.6 \pm 0.2 \times 10^{-5}$  1/Pa,  $P < 0.001$ ) and  $n$ RI increased with age ( $0.17 \pm 0.03$  vs.  $0.39 \pm 0.06$ ,  $P < 0.01$ ) for those 20–30 and 70–80 years, respectively. FCW, BCW and FDW decreased significantly with age by 86.3, 71.3 and 74.2%, respectively ( $P < 0.001$ ), all compared to the lowest age-band.

**Conclusion:** In healthy humans, ageing results in stiffer ascending aorta, with increase in  $n$ PWV and decrease in  $n$ D<sub>s</sub>. A decrease in FCW and FDW indicates decline in left ventricular early and late systolic functions with age in healthy humans with no differences between sexes.  $n$ RI is more sensitive than BCW in establishing the effects of ageing on reflected waves measured in the ascending aorta.

**Keywords:** haemodynamics, local arterial properties, magnetic resonance imaging, pulse wave velocity, wave intensity analysis

**Abbreviations:** BCW, backward compression wave;  $n$ C<sub>s</sub>, noninvasive compliance;  $n$ D<sub>s</sub>, noninvasive distensibility; FCW, forward compression wave; FDW, forward decompression wave;  $n$ PWV, noninvasive pulse wave velocity;  $n$ WIA, noninvasive wave intensity analysis

## BACKGROUND

It has long been established that pulse wave velocity (PWV) is a direct measure of arterial distensibility [1]. A large meta-analysis has shown that increased PWV predicted cardiovascular disease independently of blood pressure and other cardiovascular risk factors [2]. Additionally, PWV is an independent predictor of cardiovascular mortality [3], and fatal stroke [4] in hypertensive patients. Furthermore, PWV enhances the prediction of cardiovascular events [5], which is why most clinically used techniques for measuring arterial stiffness involve determining PWV.

Noninvasive methods for quantifying regional PWV have been explored [6–8], most commonly using the foot-to-foot method (f-t-f). The f-t-f estimates PWV as the ratio of the distance between two measurement sites at a known distance apart to the time it takes the pulse wave to travel from one site to the other; traditionally the foot of the wave. Although the carotid–femoral PWV is frequently used as an index to aortic stiffness [9], the carotid–femoral path includes segments, which have different mechanical properties and varying PWV [10,11]. Therefore, carotid–femoral PWV can only provide an average measure of stiffness over the whole pathway. Also, the path of the wave with carotid–femoral index is not unequivocal, which would lead to uncertainties.

This suggests that PWV measured locally in the ascending aorta would provide a more accurate estimation of local aortic stiffness than does regional PWV. Further, the ascending aorta is considered a prime location as it has

Journal of Hypertension 2018, 36:000–000

<sup>a</sup>King's College London, British Heart Foundation Centre, London, <sup>b</sup>Division of Experimental Medicine and Immunotherapeutics, University of Cambridge, Cambridge and <sup>c</sup>Brunel Institute for Bioengineering, Brunel University, Uxbridge, Middlesex, UK

Correspondence to Ashraf W. Khir, PhD, Brunel Institute for Bioengineering, Brunel University, Kingston Lane, Uxbridge, Middlesex UB8 3PH, UK. Tel: +44 1895265857; fax: +44 1895274608; e-mail: ashraf.khir@brunel.ac.uk

**Received** 31 January 2018 **Revised** 6 June 2018 **Accepted** 4 July 2018

J Hypertens 36:000–000 Copyright © 2018 The Author(s). Published by Wolters Kluwer Health, Inc. This is an open access article distributed under the terms of the Creative Commons Attribution-Non Commercial-No Derivatives License 4.0 (CCBY-NC-ND), where it is permissible to download and share the work provided it is properly cited. The work cannot be changed in any way or used commercially without permission from the journal.

DOI:10.1097/HJH.0000000000001886

TABLE 1. Participant characteristics

	Age groups					
	20–30 years (n = 26)	30–40 years (n = 21)	40–50 years (n = 23)	50–60 years (n = 26)	60–70 years (n = 25)	70–80 years (n = 23)
Age (years)	24 ± 3	33 ± 3	44 ± 2	57 ± 3	63 ± 2	73 ± 2
Sex (men)	11	11	9	12	11	12
BMI (kg/m <sup>2</sup> )	22.9 ± 2.7	25.9 ± 3.8	25.6 ± 4.4	23.9 ± 2.7	25.4 ± 4.0	25.0 ± 2.4
BSA (m <sup>2</sup> )	1.58 ± 0.12	1.34 ± 0.19	1.58 ± 0.14	1.50 ± 0.13	1.69 ± 0.11	1.62 ± 0.11
HR (bpm)	68 ± 11	60 ± 8	65 ± 8	66 ± 10	64 ± 9	67 ± 10
SBP (mmHg)	112 ± 13	116 ± 9	121 ± 15	117 ± 12	128 ± 16	138 ± 16
DBP (mmHg)	63 ± 5	69 ± 6	73 ± 9	71 ± 8	75 ± 6	75 ± 8

Values are means ± standard deviation (SD). BSA: body surface area; HR: heart rate; SBP: supine systolic blood pressure; DBP: supine diastolic blood pressure.

the haemodynamic conditions that are most relevant to ventricular load such as impedance [12]. Furthermore, recent reports have shown that stiffening of the proximal aorta is strongly related to ageing in healthy humans [13]; all suggesting the importance of local stiffness, although limited data are available on local stiffness within the ascending aorta [14], and especially using noninvasive direct measurements; hence the motivation of this work.

Ventricular–arterial coupling is of great clinical and physiological interest, as it provides important haemodynamic insights into the complex cardiovascular system and its changes with ageing in health and disease [15]. The wave intensity analysis (WIA) technique is most suitable for studying ventricular–arterial coupling [16] as it has been validated on the bench [17], used *in vitro* with the airways [18], *in vivo* [19] and clinical investigations [20,21], including ventricular assist devices [22]. Extensive reviews of the various applications of WIA have been provided elsewhere [23,24], but briefly WIA was initially introduced as a time-domain technique for analysing wave propagation, and the ventricular–arterial interaction [25]. Previous studies have shown that the forward compression wave (FCW) in early systole relates to left ventricular (LV) myocardial contractility, the backward compression wave (BCW) in mid-systole relates to peripheral reflections and forward decompression wave (FDW) in end-systole correlates with LV early diastolic performance [26]. Although WIA has not yet been adopted as a diagnostic tool, there is a growing number of studies that are investigating the clinical usefulness of the technique [27]. Regardless, examining the alterations of these WIA parameters, as descriptors of the ventricular–arterial coupling, with ageing, sex and disease can provide fundamental insights into the pathophysiology of cardiovascular function and could potentially improve the effectiveness of current therapeutic interventions [15].

WIA was initially derived from measurements of pressure and velocity. However, the limitation of acquiring invasive measurement of pressure prohibited the use of WIA in routine clinical settings. To avoid the need for invasive measurements, Feng and Khir [28] developed a technique for the noninvasive calculation of PWV, *n*PWV and WIA, *n*WIA, using measurements of arterial diameter and blood flow velocity, this technique has been validated *in vitro* [29] and used *in vivo* in carotid and femoral arteries [11].

In our earlier work, we examined changes of regional PWV with age [6], in this article, we extend this work to investigate local PWV in the vital location of the circulation;

ascending aorta, and further examine age-related changes of the ventricular–arterial coupling using WIA. Accordingly, the aims of this study are to determine the aortic stiffness using our noninvasive technique; demonstrate the use of noninvasive WIA; assess the ability of WIA to capture novel haemodynamic variables across the age spectrum and examine sex differences in a large population of healthy individuals, using MRI measurements.

## METHODS

### Study population

Participants were recruited from the Cambridge arm of the Anglo-Cardiff Collaborative Trial, which explores the factors influencing arterial stiffness, in a community-based investigation. Participants are free of cardiovascular disease and medication, health status were determined by medical records, and only two participants presented supine brachial blood pressure measurement greater than 140/90 mmHg. Approval was obtained from the local Research Ethics Committee, and written informed consent was obtained from all participants.

A total of 149 participants underwent haemodynamic measurements but five participants were unable to complete the MRI scan because of claustrophobia. The characteristics of the 144 participants [66 men, mean age 49 ± 17 years, mean ± standard deviation (SD), range 20–77 years] are shown in Table 1.

Brachial blood pressure of each participant was measured in duplicate in the nondominant arm, according to the British Hypertension Society Guidelines, using a validated oscillometric device (HEM-711A-E; Omron Corp., Matsusaka, Japan).

### MRI

As previously described [6], images were acquired using a 1.5T MRI system (Signa HDx; GE Healthcare, Waukesha, Wisconsin, USA). An ECG-gated, segmented *k*-space, cine phase contrast sequence (CPC-MRI) was used with the following parameters: 30° flip angle, slice thickness = 5 mm, field of view = 280 × 280 mm, repetition time = 6.7 ms, matrix = 256 × 256 and through-plane velocity encoding (VENC) = 150 cm/s, with one view per segment. In all participants, CPC-MRI sequences were performed in the ascending aorta, located approximately 1 cm distal to the aortic valve. Acquisition time was approximately 5 min for each sequence. Hundred temporal phases were

retrospectively reconstructed with a true temporal resolution of  $2 \times 6.7$  ms because of the interleaved positive and negative velocity encoding.

## Image processing

Images were analysed offline using CV Flow software (Figure S1, <http://links.lww.com/HJH/A989>, Medis, Leiden, the Netherlands). Aortic contours were automatically detected in each slice to obtain the cross-sectional area through the cardiac cycle and the area in the phase image from which the mean aortic flow velocity was calculated. Aortic diameters ( $D$ ) were calculated from the aortic areas ( $A$ ) by  $D = (4 \times A / \pi)^{1/2}$ ,  $D$  curve was smoothed using a Savitzky-Golay filter of third order with 11-point window size. The systolic ( $D_m$ ) and diastolic ( $D_0$ ) diameters were used in the analysis.

## Local noninvasive pulse wave velocity

In the absence of reflected waves in early systole,  ${}_nPWV$  ( $c$ ) can be calculated as we previously described [28]

$$c = \pm \frac{1}{2} \frac{dU_{\pm}}{d \ln D_{\pm}} \quad (1)$$

Where  $dU$  is the change in flow velocity and  $d \ln D$  is the change in the logarithmic diameter of the vessel. The '+' and '-' subscripts refer to the forward and backward travelling waves. Then, using  $c$  in the Bramwell-Hill Eq. (1) allows for determining the noninvasive distensibility ( ${}_nD_s$ ) and compliance ( ${}_nC_s$ ) as previously demonstrated [11]

$${}_nD_s = \frac{1}{\rho c^2} \quad \text{and} \quad {}_nC_s = \frac{\pi D_0^2}{4 \rho c^2} \quad (2)$$

where  $\rho$  is the blood density and assumed as  $1050 \text{ kg/m}^3$ .

The noninvasive WIA, ( ${}_n dI$ ) is calculated in the '+' and '-' directions, and as previously described [28] and can be explicitly written as

$${}_n dI_{\pm} = \pm \frac{1}{4(D/2c)} (dD \pm \frac{D}{2c} dU)^2 \quad (3)$$

The standard  ${}_n dI$  curve includes three peaks;  ${}_n dI_{+C}$  is the FCW,  ${}_n dI_{-}$  is the BCW,  ${}_n dI_{+D}$  is the FDW. Timing of peaks of FCW, BCW and FDW are  $T_n dI_{+C}$ ,  $T_n dI_{-}$  and  $T_n dI_{+D}$ . In addition, the arrival time ( $T_{rw}$ ) of BCW was also determined.  $T_{rw}$  is determined as the first sampling point of the BCW, calculated as the first minimum on the first-order derivative of the waveform. Further, we calculated the wave energies ( ${}_n I_{+C}$ ,  ${}_n I_{-}$ ,  ${}_n I_{+D}$ ) by, respectively, integrating the area under the  ${}_n dI$  three main peaks,  ${}_n dI_{+C}$ ,  ${}_n dI_{-}$ ,  ${}_n dI_{+D}$ , with respect to time. Furthermore, the ratio of BCW ( ${}_n dI_{-}$ ) to FCW ( ${}_n dI_{+C}$ ) was calculated and defined as the reflection index ( ${}_n RI$ ), as previously done [11].

## Statistics

Participant characteristics are presented as means  $\pm$  SD, results are expressed as means  $\pm$  standard error (SE). Effects of age and sex were assessed with two-way ANOVA. Post

hoc analysis was carried out using the Bonferroni method. Analysis was performed using SPSS version 22 and  $P$  less than 0.05 was taken as significant.

## RESULT

### Diameter and velocity

Figure 1a and b shows an example of flow velocity and diameter waveforms for a typical healthy participant (41-year-old man). Figure 1c illustrates the  $lnDU$ -loop used for calculating  ${}_nPWV$ , giving a result of 5.1 m/s in this case. The corresponding separated forward and backward components of flow velocity and diameter waveforms are also shown in Fig. 1d and e, as well as  ${}_nWIA$  in Fig. 1f where we can identify a FCW in early systole, followed by a BCW in mid-systole and a FDW at end of systole.

The average systolic diameters of the ascending aorta increased with age by 3.3% per decade ( $2.8 \pm 0.05$  vs.  $3.3 \pm 0.07$  cm,  $P < 0.001$ , Table 2). Men had larger ascending aorta diameters than women ( $3.2 \pm 0.05$  vs.  $3.1 \pm 0.05$  cm,  $P < 0.05$ ). Flow velocity in the ascending aorta correlated negatively with age ( $R = 0.69$ ,  $P < 0.001$ ), and men had higher values of flow velocity than women ( $0.62 \pm 0.02$  vs.  $0.54 \pm 0.02$  m/s,  $P < 0.01$ ).

### Pulse wave velocity, distensibility and compliance

As expected,  ${}_nPWV$  in the ascending aorta was significantly higher in older participants, where the average  ${}_nPWV$  across all age groups was  $5.6 \pm 0.1$  m/s, increasing linearly from  $4.7 \pm 0.3$  m/s (20–30 years) to  $6.4 \pm 0.2$  m/s (70–80 years;  $R = 0.40$ ,  $P < 0.001$ ; Fig. 2). There was no statistically significant difference between men and women.

The distensibility and compliance show the local mechanical properties of the ascending aorta. As expected, the distensibility decreased significantly with age, by 50.8% from 20–30 years old to 70–80 years old ( $P < 0.001$ ); the compliance decreased 23.2% in total ( $P < 0.001$ ). There was no significant difference in distensibility and compliance between men and women.

### Wave Intensity magnitudes and timings

FCW was decreased significantly from  $6.86 \pm 0.62 \times 10^{-5} \text{ m}^2/\text{s}$  in 20–30-year-olds to  $0.94 \pm 0.12 \times 10^{-5} \text{ m}^2/\text{s}$  in 70–80-year-olds (Fig. 3), BCW and FDW followed the same trend, decreasing from  $1.01 \pm 0.13 \times 10^{-5}$  to  $0.29 \pm 0.04 \times 10^{-5} \text{ m}^2/\text{s}$  and from  $0.89 \pm 0.08 \times 10^{-5}$  to  $0.21 \pm 0.02 \times 10^{-5} \text{ m}^2/\text{s}$ , respectively. Table 2 displays the changes of wave energies with ageing. We found no significant dependence of wave intensity and wave energy parameters on sex, except that the forward expansion wave energy ( ${}_n I_{+D}$ ) was higher in men than women ( $1.38 \pm 0.14 \times 10^{-4}$  vs.  $1.27 \pm 0.10 \times 10^{-4} \text{ m}^2$ , respectively,  $P < 0.05$ ).

The backward waveform ( $T_{rw}$ ) arrives earlier with ageing, approaching a minimum in late life ( $57 \pm 3$  ms at 20–30 years old vs.  $43 \pm 3$  ms at 70–80 years old). Interestingly, the timing of peak of  ${}_n dI_{-}$  was greater with increasing age, from  $80 \pm 10$  ms in 20–30-year-olds to  $193 \pm 33$  ms in 70–80-year-olds ( $P < 0.001$ ).

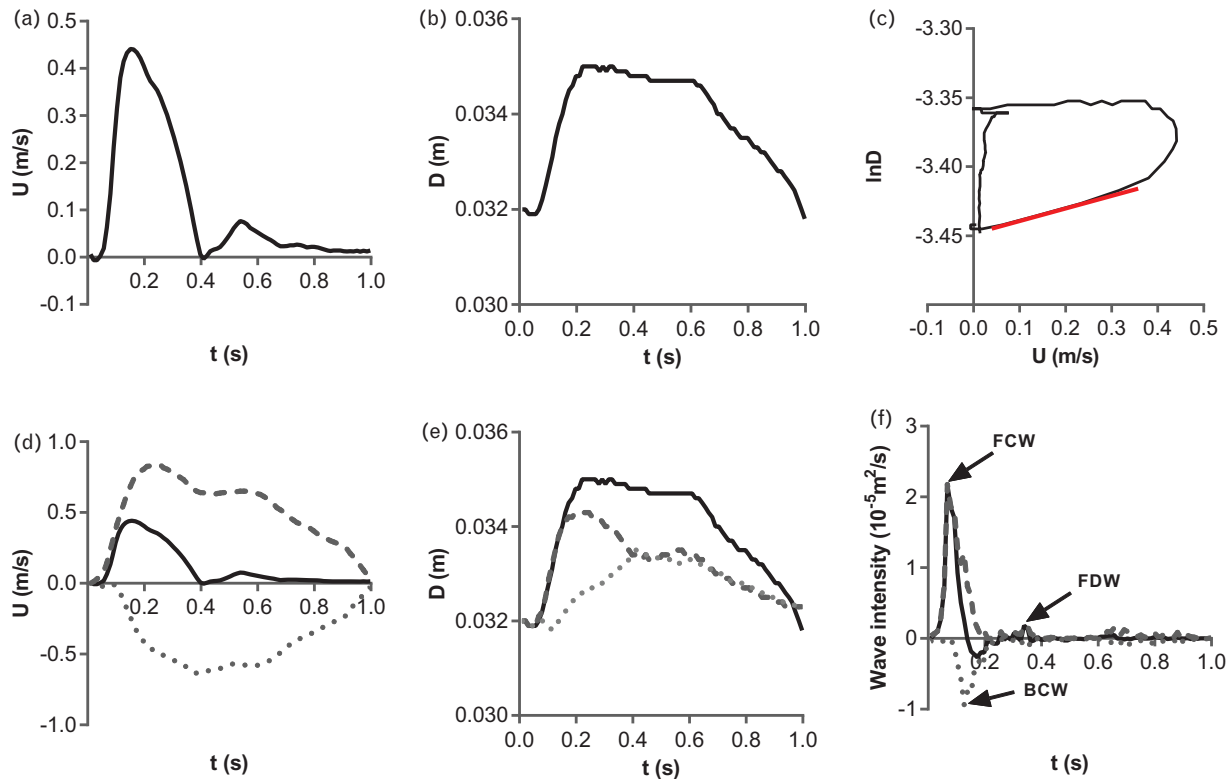


**FIGURE 1** Determination of pulse wave velocity, and the separation of waves. Diameter (a) and flow velocity (b) measured in the ascending aorta of a typical healthy participant (male participant, age 41), using MRI. In early systole, the relationship between the velocity and logarithm of diameter is linear, as shown in the initial part of the  $\ln D$ -loop (c) and the slope (highlighted in red) of which indicates local PWV of 5.1 m/s as calculated using Eq. (1). Using knowledge of PWV with  $dU$  and  $d\ln D$  data, the net, forward (dashed) and backward (dotted) wave intensity were calculated using Eq. (3) and finally plotted against time (f). PWV, pulse wave velocity.

$\rho$ RI, indicating wave reflections, increased with age, from  $0.17 \pm 0.03$  in 20–30-year-olds to  $0.39 \pm 0.06$  in 70–80-year-olds ( $P < 0.005$ ), but was not significantly affected by sex.

## DISCUSSION

Using phase contrast magnetic resonance (MR) imaging, we have demonstrated the feasibility of determining local

**TABLE 2. Noninvasive wave intensity analysis for all age groups**

Parameters	Age groups						P value
	20–30 years (n = 26)	30–40 years (n = 21)	40–50 years (n = 23)	50–60 years (n = 26)	60–70 years (n = 25)	70–80 years (n = 23)	
$\rho$ PWV (m/s)	$4.7 \pm 0.3$	$5.2 \pm 0.3$	$5.6 \pm 0.3$	$5.9 \pm 0.3$	$6.1 \pm 0.3$	$6.4 \pm 0.3$	0.001
$\rho D_s$ ( $10^{-5}$ 1/Pa)	$5.3 \pm 0.51$	$4.2 \pm 0.49$	$4.1 \pm 0.58$	$3.2 \pm 0.34$	$3.2 \pm 0.38$	$2.6 \pm 0.24$	0.001
$\rho C_s$ ( $10^{-8}$ m <sup>2</sup> /Pa)	$2.6 \pm 0.32$	$2.5 \pm 0.32$	$2.7 \pm 0.33$	$2.3 \pm 0.24$	$2.4 \pm 0.29$	$2.0 \pm 0.17$	0.644
$D_m$ (cm)	$2.8 \pm 0.07$	$3.0 \pm 0.07$	$3.2 \pm 0.09$	$3.2 \pm 0.08$	$3.3 \pm 0.08$	$3.3 \pm 0.07$	0.001
$D_0$ (cm)	$2.5 \pm 0.05$	$2.7 \pm 0.07$	$3.0 \pm 0.09$	$2.9 \pm 0.09$	$3.1 \pm 0.07$	$3.1 \pm 0.07$	<0.001
$U$ (m/s)	$0.8 \pm 0.03$	$0.7 \pm 0.04$	$0.6 \pm 0.03$	$0.5 \pm 0.03$	$0.5 \pm 0.02$	$0.4 \pm 0.02$	0.001
FCW ( $10^{-5}$ m <sup>2</sup> /s)	$6.9 \pm 0.6$	$4.1 \pm 0.5$	$3.2 \pm 0.4$	$2.0 \pm 0.3$	$1.7 \pm 0.2$	$0.9 \pm 0.1$	0.001
BCW ( $10^{-5}$ m <sup>2</sup> /s)	$-1.0 \pm 0.13$	$-0.9 \pm 0.16$	$-0.6 \pm 0.13$	$-0.4 \pm 0.04$	$-0.3 \pm 0.03$	$-0.3 \pm 0.04$	0.001
FDW ( $10^{-5}$ m <sup>2</sup> /s)	$0.9 \pm 0.08$	$0.5 \pm 0.08$	$0.4 \pm 0.06$	$0.3 \pm 0.02$	$0.3 \pm 0.03$	$0.2 \pm 0.02$	0.001
$\rho_{+C}$ ( $10^{-4}$ m <sup>2</sup> )	$2.7 \pm 0.18$	$1.8 \pm 0.17$	$1.3 \pm 0.14$	$0.8 \pm 0.09$	$0.7 \pm 0.08$	$0.5 \pm 0.07$	0.001
$\rho_{-}$ ( $10^{-4}$ m <sup>2</sup> )	$-1.0 \pm 0.12$	$-0.9 \pm 0.13$	$-0.6 \pm 0.08$	$-0.4 \pm 0.03$	$-0.4 \pm 0.03$	$-0.3 \pm 0.04$	0.001
$\rho_{+D}$ ( $10^{-4}$ m <sup>2</sup> )	$0.7 \pm 0.07$	$0.4 \pm 0.07$	$0.3 \pm 0.03$	$0.2 \pm 0.02$	$0.2 \pm 0.01$	$0.2 \pm 0.02$	0.001
$\rho$ RI	$0.17 \pm 0.03$	$0.24 \pm 0.03$	$0.21 \pm 0.03$	$0.19 \pm 0.02$	$0.28 \pm 0.05$	$0.39 \pm 0.06$	0.002
$T_{\rho}d_{+C}$ (ms)	$29 \pm 3$	$44 \pm 5$	$39 \pm 6$	$41 \pm 6$	$42 \pm 5$	$49 \pm 11$	0.357
$T_{\rho}d_{+D}$ (ms)	$303 \pm 14$	$397 \pm 29$	$311 \pm 25$	$332 \pm 15$	$351 \pm 35$	$325 \pm 30$	0.157
$T_{\rho}d_{-}$ (ms)	$80 \pm 10$	$95 \pm 8$	$114 \pm 11$	$126 \pm 14$	$189 \pm 32$	$193 \pm 33$	0.001
$T_{\rho w}$ (ms)	$57 \pm 3$	$54 \pm 3$	$50 \pm 4$	$44 \pm 5$	$47 \pm 4$	$43 \pm 3$	0.069

Values are means  $\pm$  standard error. BCW, peak of backward compression wave;  $D_m$ , systolic diameter;  $D_0$ , diastolic diameter; FCW, peak of forward compression wave; FDW, peak of forward decomposition wave;  $\rho C_s$ , noninvasive compliance;  $\rho D_s$ , noninvasive distensibility;  $\rho_{-}$ , BCW energy;  $\rho_{+C}$ , forward compression wave energy;  $\rho_{+D}$ , forward decomposition wave energy;  $\rho$ RI, noninvasive reflection index calculated by ratio of BCW to FCW; PWV, pulse wave velocity;  $T_{\rho}d_{-}$ , timing of BCW;  $T_{\rho}d_{+C}$ , timing of FCW;  $T_{\rho}d_{+D}$ , timing of FDW;  $T_{\rho w}$ , arrival time of backward wave.

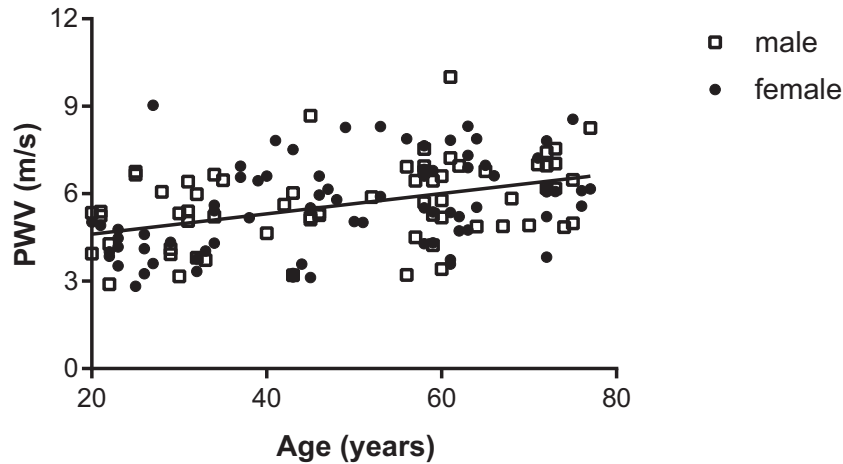


**FIGURE 2** Relationship between age and ascending aorta pulse wave velocity for all participants, linear data fitting ( $R=0.40$ ,  $P<0.001$ ).

$n$ PWV,  $nD_s$  and  $n$ dI in the human ascending aorta from direct measurements of diameter and blood flow velocity. Wave intensity parameters and reflection index were also calculated (Figs 3 and 4). In addition, and for the first time, we have investigated the effect of age and sex on these parameters in a healthy population covering a wide age-spectrum. The main findings of the current study were: ascending aorta  $n$ PWV and  $nD_s$  increased and decreased with age, respectively; the magnitude of FCW, FDW and BCW decreased, but the  $n$ RI increased with age; the arrival time of BCW decreased with age.

In the current work, local  $n$ PWV is derived from MRI measurement at a single point in the ascending aorta (aortic root) being a prominent location in the circulation; because of its proximity and direct influence on ventricular performance. This allowed also for the noninvasive determination of the ascending aorta distensibility, a widely used parameter for characterizing arterial stiffness. The MRI-based technique is both useful and convenient as pressure measurement is not required or assumed in the calculation, highlighting the potential contribution of the current method and findings.

There are numerous studies addressing the age-related changes in regional PWV measured using the f-t-f method. Although this technique is well established, with many commercial devices available, at best it only provides a regional average of the PWV, which varies locally because of the varying dimensions and wall properties along the arterial path. Moreover, different segments of the path undergo different changes with ageing and disease, which complicates the interpretation [30]. Those regional indices also have inherent problems related to exclusion of the proximal aorta from the path length (the proximal aorta normally contributes  $\sim 50\%$  of total arterial compliance) [31], and the uncertainty of the distance travelled by the pulse wave [32]. The latter is particularly problematic in older individuals where there is greater tortuosity of the arterial tree [33]. Table 2 of Hickson *et al.* [6], indicates a difference as large as 28% between PWV measured along the aorta using MRI and carotid–femoral index using SpymcoCor ( $5.7 \pm 1.8$  vs.  $7.3 \pm 1.8$  m/s,  $R=0.71$ ,  $P<0.001$ ). However, local  $n$ PWV determined in the current

study is derived from MRI measurement at a single point and could theoretically be performed at any other location along the arterial system.

Compliance and distensibility are common measures of arterial stiffness. Compliance is determined as the change of segmental volume ( $\Delta V$ ) in response to change in blood pressure ( $\Delta P$ ), which requires the invasive measurement of pressure. Distensibility on the other hand is preferred as it is normalized to the initial segmental volume ( $V$ ) and allows for comparisons between different sized vessels and/or participants, and has been found to relate more closely to arterial wall stiffness [34]. As expected, in the current study the distensibility of the ascending aorta decreased with age (Fig. 4), in agreement with previous reports [13]. We found that the impact of age was most marked in those more than 50 years of age;  $nD_s$  decreased in 50–60, 60–70 and 70–80-year-olds, by 39.5, 40.2 and 50.8%, respectively.

Utilizing MRI, Vulliémoz *et al.* [35], with direct measurements of flow ( $Q$ ) and area ( $Q$ ), QA-method, reported PWV values of 4.9 m/s, which is in agreement with our results of 5.4 m/s in the ascending aorta. Also utilizing MRI, Biglino *et al.* [36], developed a variation of our initial derivation [28,37] and calculated  $n$ PWV and  $n$ WIA using measurements of velocity and vessel area (rather than diameter). The authors reported PWV of 5.8 m/s in the ascending aorta, which is in good agreement with our result at approximately the same location. This variation has also been used in pulmonary hypertension [38], all demonstrating that  $n$ WIA provides a valid alternative to invasive WIA and offers a description of the coupling between the ejecting ventricle and the arterial bed, through its three main peaks; FCW, FDW and BCW.

Classical approaches for the separation of pressure and velocity waveforms to their forward and backward directions have been introduced in the frequency [39] and time [40] domains. Different techniques for the determination of the reflection index have been tested *in vitro* [41] and used *in vivo* [11] using pressure and velocity, or diameter and velocity approaches. The reflection index ( $n$ RI) in this study is calculated as the ratio of BCW over FCW and the average values of each decade reported in Table 2 show that  $n$ RI significantly increased with age ( $P=0.002$ ). As pressure

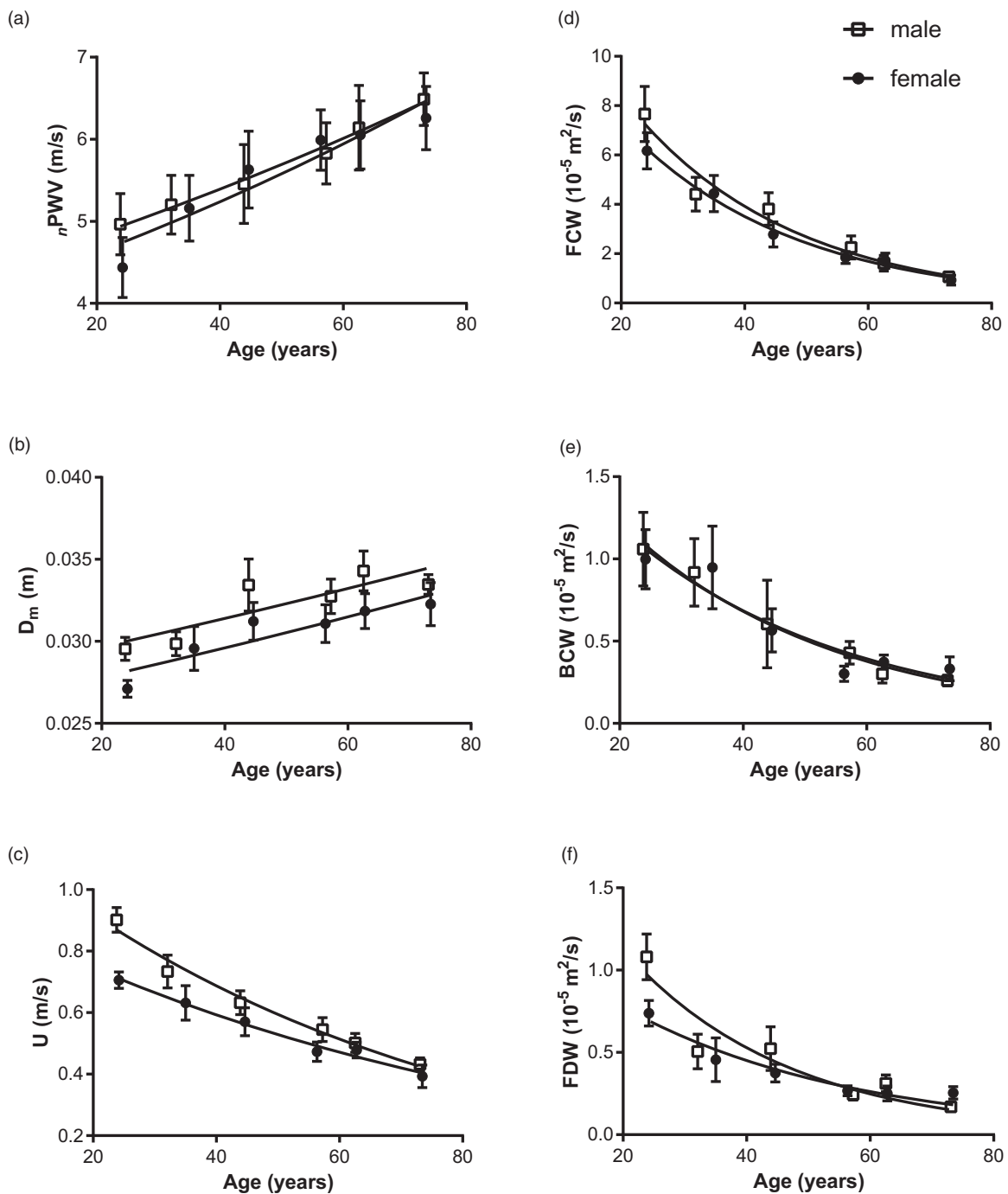


**FIGURE 3** Local pulse wave velocity (a), diameter (b), flow velocity (c), forward compression wave; backward compression wave (d), backward compression wave (e) and forward decompression wave (f) are shown as a function of age with sex. BCW, backward compression wave; FCW, forward compression wave; FDW, forward decompression wave.

measurements were not taken in this study, we also calculated the reflection index using the separated flow velocity and separately, using the diameter waveforms as the ratio of peak backward velocity to peak forward velocity, and peak backward diameter to forward diameter. The separated waves techniques have also shown to increase with age. Although the absolute values of these reflection indices do not produce similar values as they use different fundamental units, they all share the same trend of increase with age.

Earlier work demonstrated that aortic FCW is proportional to left ventricular myocardial contractility (max  $dP/dt$ ) [42], thus FCW may provide an alternative way to assess LV function, which declines with age in the current study. Further, aortic BCW indicates discontinuities and reflection sites in the proximal arteries, and importantly, can provide novel haemodynamic information concerning aortic stenosis and aneurysm [19,38]. However, the magnitude of BCW decreased with age in our study, which was surprising. A

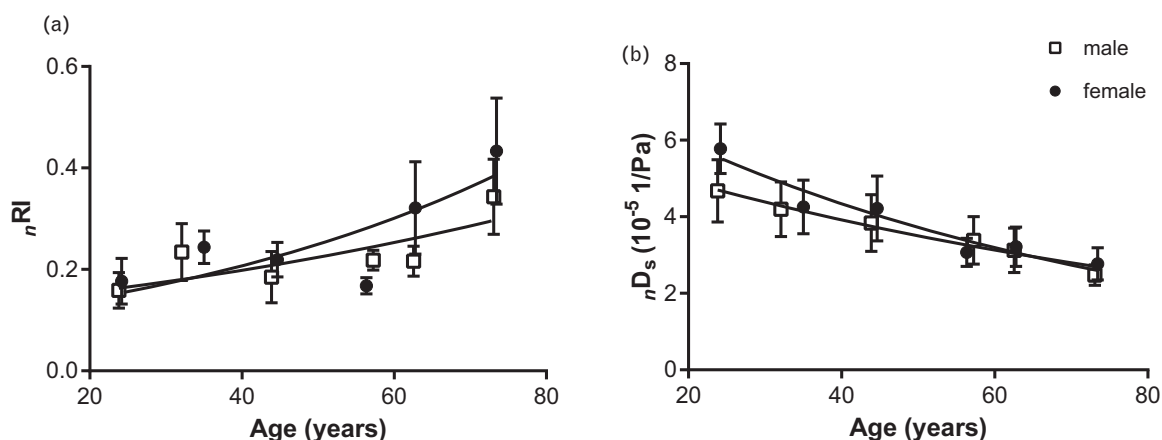


**FIGURE 4** Reflection index (a) and distensibility (b) are shown as a function of age and sex.  $rRI$  increased but distensibility decreased with age for both sexes.  $rRI$ , reflection index.

possible explanation for this result is the reduction of the FCW magnitude with age, and that the BCW had to follow the same pattern. We note that  $rRI$  was more sensitive and indeed increased with age, suggesting that it is the ratio of the BCW to the FCW, and not the absolute value of the BCW, that better describes the stiffening of the arterial system.

The arrival time of BCW was associated with ventricular hypertrophy and heart failure in patients [43]. The findings in the current study demonstrate that increased PWV because of reduced distensibility, resulted in earlier arrival of BCW in older groups. These results clearly indicate stiffening of the arterial system with age even in healthy individuals, which resulted in an increase in ventricular load and decline in ventricular performance, judged by the reduction in FCW and FDW, as previously suggested [26].

Our results obtained using MRI show significant differences in the magnitude of FCW and FDW, and the timing of peak BCW between older and younger participants, which agree with earlier reports in the carotid artery using ultrasound [11]. Both, the current MRI results and earlier work using ultrasound have shown that the technique is sensitive to changes in age, thus demonstrating the potential clinical applications of  $nWIA$  [26].

An increase in regional PWV has been reported as a surrogate marker for cardiovascular events [44–46]. Therefore, we extrapolate that the increase of local PWV in the ascending aorta could potentially be used as a clinical predictor to cardiovascular events. Further, the elasticity of the ascending aorta is an important parameter in determining left ventricular afterload, and the distensibility measurement in ascending aorta could also be used to evaluate the influence of the ascending mechanical properties on systolic ventricular function and the vascular-ventricular coupling through the FCW, FDW and BCW. Therefore, the results of this study provide plausible insights into the effects of ageing on the ascending aorta haemodynamics and their effects on ventricular function with ageing.

### Limitation

The CPC-MRI sequence that we used was suboptimal to measure diastolic diameter accurately, therefore, the

absolute values of compliance calculated in this study may be less accurate than those that could have been obtained if a faster sequence had been used. Regardless, this is not expected to change the overall trend or differences in compliance with age or between sexes, and thus does not alter our conclusions. Further, although the sampling frequency was not as high as what could potentially be acquired with ultrasound, MRI provided data that facilitated the analysis to capture local waves in the ascending aorta.

In conclusion, we demonstrated that local PWV, distensibility and noninvasive WIA parameters as well as the reflection index can feasibly be calculated in the ascending aorta using CPC-MRI. The MRI fundamental measurements provided the basis for a description of the coupling between the ejecting ventricle and the arterial bed, using  $nWIA$ .

In healthy adults, local ascending aorta PWV increased and distensibility decreased with age, with no significant difference between men and women. The decrease in the forward compression and decompression waves indicates a decline in LV function with age, even in healthy individuals. The reflection index is more sensitive than the magnitude of the BCW in establishing the effects of ageing on reflected waves measured in the ascending aorta

## Perspectives

### Competency in medical knowledge

Aortic PWV is a direct measurement of aortic distensibility/stiffness. The current recommended method for determining aortic PWV is complex, requiring measurements of pressure or flow velocity at two different locations and an estimated distance between them. Alternatively, the same information could be achieved from using CPC-MRI with measurements of diameter and velocity at single location.

### Translational outlook

The determination of noninvasive local PWV and WIA in the ascending aorta as demonstrated in this study is useful for evaluating arterial distensibility/stiffness and the ventricular–arterial coupling, respectively. These parameters

could potentially be implemented in routine MR examinations, providing further information that could assist in the diagnosis and guide therapeutic strategies.

## ACKNOWLEDGEMENTS

### Conflicts of interest

There are no conflicts of interest.

## REFERENCES

- Bramwell JC, Hill AV. The velocity of the pulse wave in man. *Proc R Soc B Biol Sci* 1922; 93:298–306.
- Blacher J, Asmar R, Djane S, London GM, Safar ME. Aortic pulse wave velocity as a marker of cardiovascular risk in hypertensive patients. *Hypertension* 1999; 33:1111–1117.
- Laurent S, Boutouyrie P, Asmar R, Gautier I, Laloux B, Guize L, et al. Aortic stiffness is an independent predictor of all-cause and cardiovascular mortality in hypertensive patients. *Hypertension* 2001; 37:1236–1241.
- Laurent S, Katsahian S, Fassot C, Tropeano AI, Gautier I, Laloux B, et al. Aortic stiffness is an independent predictor of fatal stroke in essential hypertension. *Stroke* 2003; 34:1203–1206.
- Ben-Shlomo Y, Spears M, Boustred C, May M, Anderson SG, Benjamin EJ, et al. Aortic pulse wave velocity improves cardiovascular event prediction: an individual participant meta-analysis of prospective observational data from 17,635 subjects. *J Am Coll Cardiol* 2014; 63:636–646.
- Hickson SS, Butlin M, Graves M, Taviani V, Avolio AP, McEniery CM, et al. The relationship of age with regional aortic stiffness and diameter. *JACC Cardiovasc Imaging* 2010; 3:1247–1255.
- Rogers WJ, Hu YL, Coast D, Vido DA, Kramer CM, Pyeritz RE, et al. Age-associated changes in regional aortic pulse wave velocity. *J Am Coll Cardiol* 2001; 38:1123–1129.
- Dogui A, Redheuil A, Lefort M, Decesare A, Kachenoura N, Herment A, et al. Measurement of aortic arch pulse wave velocity in cardiovascular MR: Comparison of transit time estimators and description of a new approach. *J Magn Reson Imaging* 2011; 33:1321–1329.
- Millasseau SC, Stewart AD, Patel SJ, Redwood SR, Chowienczyk PJ. Evaluation of carotid-femoral pulse wave velocity: Influence of timing algorithm and heart rate. *Hypertension* 2005; 45:222–226.
- Khiri AW, Zambanini A, Parker KH. Local and regional wave speed in the aorta: effects of arterial occlusion. *Med Eng Phys* 2004; 26:23–29.
- Borlotti A, Khiri AW, Rietzschel ER, De Buyzere ML, Vermeersch S, Segers P. Noninvasive determination of local pulse wave velocity and wave intensity: changes with age and gender in the carotid and femoral arteries of healthy human. *J Appl Physiol (1985)* 2012; 113:727–735.
- Adji A, Kachenoura N, Bollache E, Avolio A, O'Rourke M, Mousseaux E. Magnetic resonance and applanation tonometry for noninvasive determination of left ventricular load and ventricular vascular coupling in the time and frequency domain. *J Hypertens* 2016; 34:1099–1108.
- Redheuil A, Yu WC, Wu CO, Mousseaux E, De Cesare A, Yan R, et al. Reduced ascending aortic strain and distensibility: Earliest manifestations of vascular aging in humans. *Hypertension* 2010; 55:319–326.
- Nethononda RM, Lewandowski AJ, Stewart R, Kyliantiras I, Whitworth P, Francis J, et al. Gender specific patterns of age-related decline in aortic stiffness: a cardiovascular magnetic resonance study including normal ranges. *J Cardiovasc Magn Reson* 2015; 17:20.
- Chantler PD, Lakatta EG. Arterial-ventricular coupling with aging and disease. *Front Physiol* 2012; 3:90.
- Ramsey MW, Sugawara M. Arterial wave intensity and ventriculoarterial interaction. *Heart Vessel (Suppl 12)*:1997;128–134.
- Khiri AW, Parker KH. Measurements of wave speed and reflected waves in elastic tubes and bifurcations. *J Biomech* 2002; 35:775–783.
- Clavica F, Parker KH, Khiri AW. Wave intensity analysis in air-filled flexible vessels. *J Biomech* 2015; 48:687–694.
- Khiri AW, Parker KH. Wave intensity in the ascending aorta: effects of arterial occlusion. *J Biomech* 2005; 38:647–655.
- Li Y, Gu H, Alastruey J, Chowienczyk P. Forward and backward pressure waveform morphology in hypertension. *Hypertension* 2017; 69:375–381.
- Khiri AW, Henein MY, Koh T, Das SK, Parker KH, Gibson DG. Arterial waves in humans during peripheral vascular surgery. *Clin Sci (Lond)* 2001; 101:749–757.
- Kolyva C, Pantalos GM, Giridharan G a, Pepper JR, Khiri AW. Discerning aortic waves during intra-aortic balloon pumping and their relation to benefits of counterpulsation in humans. *J Appl Physiol (1985)* 2009; 107:1497–1503.
- Kolyva C, Khiri AW. Wave intensity analysis in the great arteries - what has been learned in the past 25 years? Part I. *ICFJ* 2013; 1:68–73.
- Kolyva C, Khiri AW. Wave intensity analysis in the ventricles, carotid and coronary arteries – what has been learnt during the last 25 years?: part 2. *ICFJ* 2014; 1:122–127.
- Parker KH, Jones CJ, Dawson JR, Gibson DG. What stops the flow of blood from the heart? *Heart Vessels* 1988; 4:241–245.
- Ohte N, Narita H, Sugawara M, Niki K, Okada T, Harada A, et al. Clinical usefulness of carotid arterial wave intensity in assessing left ventricular systolic and early diastolic performance. *Heart Vessels* 2003; 18:107–111.
- Sugawara M, Niki K, Ohte N, Okada T, Harada A. Clinical usefulness of wave intensity analysis. *Med Biol Eng Comput* 2009; 47:197–206.
- Feng J, Khiri AW. Determination of wave speed and wave separation in the arteries using diameter and velocity. *J Biomech* 2010; 43:455–462.
- Li Y, Khiri AW. Experimental validation of noninvasive and fluid density independent methods for the determination of local wave speed and arrival time of reflected wave. *J Biomech* 2011; 44:1393–1399.
- Cameron JD, Bulpitt CJ, Pinto ES, Rajkumar C. The aging of elastic and muscular arteries: a comparison of diabetic and nondiabetic subjects. *Diabetes Care* 2003; 26:2133–2138.
- Ioannou CV, Stergiopoulos N, Katsamouris AN, Startchik I, Kalangos A, Licker MJ, et al. Hemodynamics induced after acute reduction of proximal thoracic aorta compliance. *Eur J Vasc Endovasc Surg* 2003; 26:195–204.
- Weber T, Ammer M, Rammer M, Adji A, O'Rourke MF, Wassertheurer S, et al. Noninvasive determination of carotid-femoral pulse wave velocity depends critically on assessment of travel distance: a comparison with invasive measurement. *J Hypertens* 2009; 27:1624–1630.
- Sugawara J, Hayashi K, Yokoi T, Tanaka H. Age-associated elongation of the ascending aorta in adults. *JACC Cardiovasc Imaging* 2008; 1:739–748.
- Cecelja M, Chowienczyk P. Role of arterial stiffness in cardiovascular disease. *JRSM Cardiovasc Dis* 2012; 1; pii: cvd.2012.012016.
- Vulliémot S, Stergiopoulos N, Meuli R. Estimation of local aortic elastic properties with MRI. *Magn Reson Med* 2002; 47:649–654.
- Biglino G, Steeden JA, Baker C, Schievano S, Taylor AM, Parker KH, et al. A noninvasive clinical application of wave intensity analysis based on ultrahigh temporal resolution phase-contrast cardiovascular magnetic resonance. *J Cardiovasc Magn Reson* 2012; 14:57.
- Feng J, Khiri AW. Determination of wave intensity in flexible tubes using measured diameter and velocity. *Conf Proc IEEE Eng Med Biol Soc* 2007; 2007:985–988.
- Quail MA, Knight DS, Steeden JA, Taelman L, Moledina S, Taylor AM, et al. Noninvasive pulmonary artery wave intensity analysis in pulmonary hypertension. *AJP Hear Circ Physiol* 2015; 308:H1603–H1611.
- Westerhof N, Sipkema P, Bos GC, Van Den Elzinga G. Forward and backward waves in the arterial system. *Cardiovasc Res* 1972; 6:648–656.
- Parker KH, Jones CJ. Forward and backward running waves in the arteries: analysis using the method of characteristics. *J Biomech Eng* 1990; 112:322–326.
- Li Y, Borlotti A, Hickson SS, McEniery CM, Wilkinson IB, Khiri AW. Using magnetic resonance imaging measurements for the determination of local wave speed and arrival time of reflected waves in human ascending aorta. In: 2010 Annual International Conference of the IEEE Engineering in Medicine and Biology Society, EMBC'10. 2010. pp. 5153–5156.
- Niki K, Sugawara M, Uchida K, Tanaka R, Tanimoto K, Imamura H, et al. A noninvasive method of measuring wave intensity, a new hemodynamic index: application to the carotid artery in patients with mitral regurgitation before and after surgery. *Heart Vessels* 1999; 14:263–271.

43. Koh TW, Pepper JR, DeSouza AC, Parker KH. Analysis of wave reflections in the arterial system using wave intensity: A novel method for predicting the timing and amplitude of reflected waves. *Heart Vessels* 1998; 13:103–113.
44. Maroules CD, Khera A, Ayers C, Goel A, Peshock RM, Abbara S, *et al.* Cardiovascular outcome associations among cardiovascular magnetic resonance measures of arterial stiffness: the Dallas heart study. *J Cardiovasc Magn Reson* 2014; 16:33.
45. Vlachopoulos C, Aznaouridis K, Stefanadis C. Prediction of cardiovascular events and all-cause mortality with arterial stiffness. *J Am Coll Cardiol* 2010; 55:1318–1327.
46. Ohyama Y, Ambale-Venkatesh B, Noda C, Kim J-Y, Tanami Y, Teixido-Tura G, *et al.* Aortic arch pulse wave velocity assessed by magnetic resonance imaging as a predictor of incident cardiovascular events: the MESA (Multi-Ethnic Study of Atherosclerosis). *Hypertension* 2017; 70:524–530.